Article

Comparison of a MEMS-Based Handheld OCT Scanner With a Commercial Desktop OCT System for Retinal Evaluation

Samir I. Sayegh[1] ✉, Ryan M. Nolan[2], Woonggyu Jung[3], Jeehyun Kim[4], Daniel T. McCormick[5], Eric J. Chaney[2], Charles N. Stewart[6], and Stephen A. Boppart[2,7]

[1] The Eye Center, Champaign, IL, USA
[2] Beckman Institute for Advanced Science and Technology, Urbana, IL, USA
[3] School of Nano-Bioscience and Chemical Engineering, Ulsan National Institute of Science and Technology, Korea
[4] Department of Electrical and Computer Engineering, Kyungpook National University, Korea
[5] AdvancedMEMS, San Francisco, CA, USA
[6] Welch Allyn, Inc., Skaneateles Falls, NY, USA
[7] Departments of Electrical and Computer Engineering, Bioengineering, and Internal Medicine, University of Illinois at Urbana-Champaign, Urbana, IL, USA

Purpose: The goal of this study was to evaluate the ability of our handheld optical coherence tomography (OCT) scanner to image the posterior and anterior structures of the human eye, and especially the individual layers of the retina, and to compare its diagnostic performance with that of a fixed desktop commercial ophthalmic OCT system.

Methods: We compared the clinical imaging results of our handheld OCT with a leading commercial desktop ophthalmic system (RTVue) used in specialist offices. Six patients exhibiting diabetes-related retinal pathology had both eyes imaged with each OCT system.

Results: In both sets of images, the structural irregularities of the retinal layers could be identified such as retinal edema and vitreomacular traction.

Conclusions: Our handheld OCT system can be used to identify relevant anatomical structures and pathologies in the eye, potentially enabling earlier screening, disease detection, and treatment. Images can be acquired quickly, with sufficient resolution and negligible motion artifacts that would normally limit its diagnostic use.

Translational Relevance: Following screening and early disease detection in primary care via our optimized handheld OCT system, patients can be referred to a specialist for treatment, preventing further disease progression. While many primary care physicians are adept at using the ophthalmoscope, they can definitely take advantage of more advanced technologies.

Introduction

Optical coherence tomography (OCT) is an established high-resolution modality capable of in vivo, noninvasive, cross-sectional, real-time imaging.[1] Ophthalmology is the most dominant clinical application for OCT, where large commercial desktop systems and laboratory-based research systems have been extensively used.[2–6] With the advent of microelectronics, micro-optics, and microelectromechanical systems (MEMS) scanners,[7–12] OCT systems can be constructed as compact, portable, and cost-effective devices with handheld scanners to accommodate the needs of specialists, as well as primary care physicians.[13] Practically, physicians across all specialties need to be able to easily maneuver a system in the limited available space of an examination room and between rooms. Advancing to address this need, we have developed an OCT system suitable for primary care imaging, as well as many other medical and surgical specialties.[13] This system has been used in feasibility studies to examine the tissue sites commonly examined by primary care physicians including the eye, ear, oral mucosa, and skin.[14]
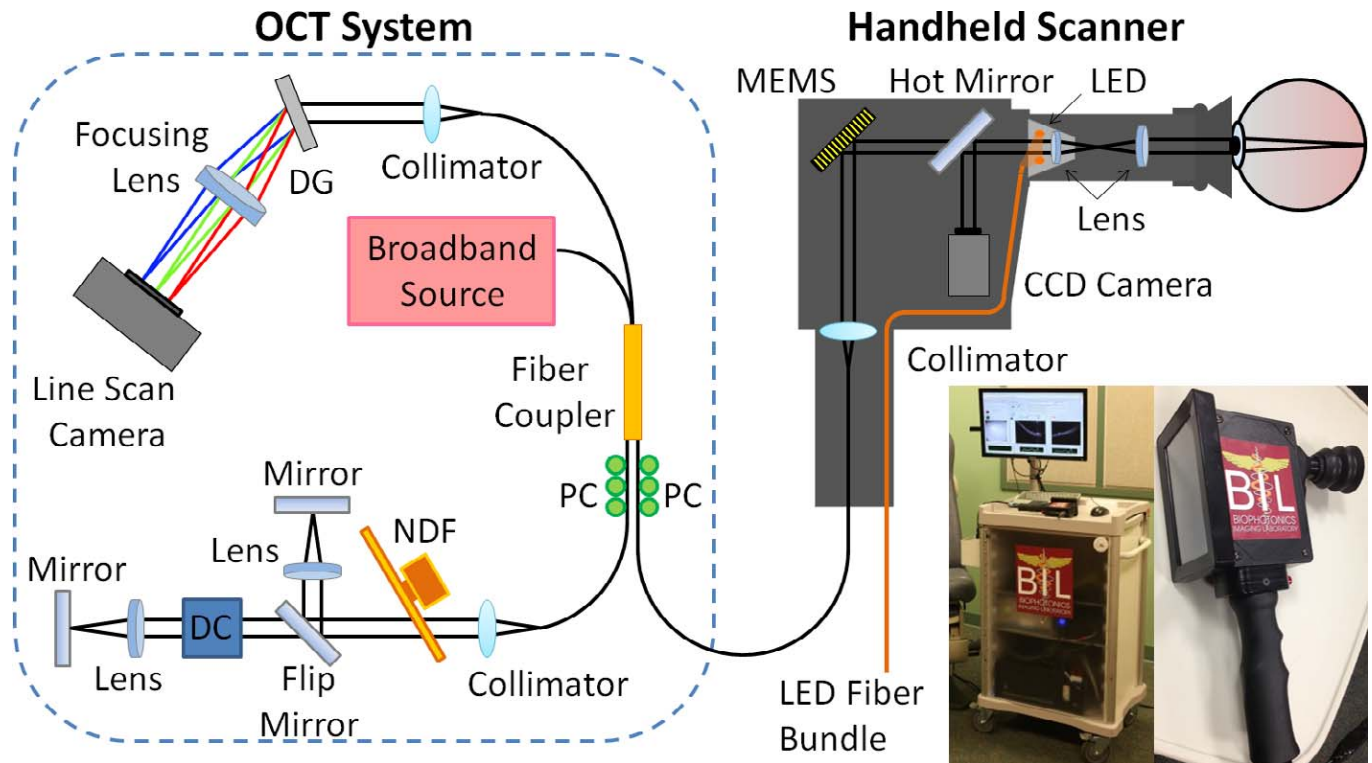
Figure 1. Schematic diagram and photograph of the portable OCT system and handheld scanner equipped with the interchangeable lens mounts for corneal or retinal imaging. *Abbreviations*: DG, diffraction grating; PC, polarization controller; NDF, neutral density filter; DC, dispersion compensation unit.

In the United States, currently one in ten Americans has diabetes, and one in four does not know it. If current trends hold, one in three Americans will have diabetes by 2050.[15] Diabetic retinopathy is the leading cause of blindness in individuals younger than age 75.[16] The worldwide trend is equally worrisome. A number of screening, diagnostic, and interventional measures need to be put in place to control the disease and its sequela. For most patients, the first encounter with a medical provider is most likely to be at the primary care level. It is essential, therefore, to place the appropriate screening and diagnostic tools in the hands of these healthcare providers. Early diagnosis is especially relevant since there are now more effective therapeutic modalities. Studies such as the Early Treatment Diabetic Retinopathy Study (ETDRS), and a Study of Ranibizumab Injection in Subjects With Clinically Significant Macular Edema (ME) With Center Involvement Secondary to Diabetes Mellitus the clinical trial numbers RISE (NCT00473330) and RIDE (NCT00473382) have consistently demonstrated the positive effect of early treatment in diabetic macular edema.[17,18] Simplified classification systems and reliance on OCT for quantitative three-dimensional (3D) characterization of retinal edema have seen an increasing trend.[2,3,19–24] Corneal applications, especially for monitoring refractive surgery outcomes, are important[25–31] but will be discussed in a separate article.

Due to the increasingly important role that OCT has in ophthalmology, the goal of this study was to evaluate the performance of our handheld OCT scanner at imaging microstructures in the human retina, and directly compare images of healthy and pathological tissue with those acquired with a commercial desktop ophthalmic OCT system, captured from the same anatomical locations on the same patients.

Materials and Methods

Our handheld scanner was specifically designed to rapidly acquire patient images at 70,422 A-scans/sec (~70 frames/sec and ~1000 axial A-scans/image) with 4-μm axial resolution and 15-μm transverse resolution in tissue. To our knowledge, this is the fastest acquisition rate of any handheld OCT system, at time of submission. In our OCT system (Fig. 1), the handheld scanner consists of a collimator, MEMS scanning mirror, dichroic mirror, and a compact color

Table 1. OCT System Specification Comparison Between Our Handheld OCT Scanner System and a Leading Commercial Desktop Ophthalmic System (RTVue, Optovue, Inc.[32])

		Handheld	Desktop
Scanner	OCT image (A-scans/sec)	70,422	26,000
	Frame rate (A-scans/frame)	1,006 (70 frames/sec)	256–1,024 (25–101 frames/sec)
	Depth resolution, μm	4	5
	Transverse resolution, μm	15 (undilated)	8 (undilated)
Scan range	Depth, mm	2	2–2.3
Scan beam wavelength	λ, nm	830	840
Exposure power at pupil	mW	1	0.75
OCT fundus image (en face)	FOV, deg (H × V)	10 × 10	32 × 22
	Minimum pupil diameter, mm	2.5	2.5
External image (live IR)	FOV, mm^2	3 × 3	13 × 9[a]
Computer	CPU	2.83 GHz quad-core processor	2.66 GHz quad-core processor

[a]RTVue images were acquired at the standard system settings: 8 × 8 mm^2 (retinal) and 6 × 6 mm^2 (corneal).

charge-coupled device (CCD) video camera (0.27 megapixel) with light-emitting diode (LED) fiber-optic illumination in a light and robust plastic box (11.5 × 11.5 × 6.3 cm^3).

The CCD camera allows for viewing of the anterior and posterior chambers of the patient's eye, similar to an ophthalmoscope, and enables precise positioning of the OCT beam over small areas of interest, while simultaneously and synchronously capturing video images of tissue surface features during OCT image acquisition. Interchangeable lens mounts equipped with a soft eyecup were designed and optimized for use during corneal and retinal imaging.[13] The reference arm was constructed with two different and selectable optical paths, a short optical path for corneal imaging and a long path for retinal imaging. These paths are easily interchanged using a magnetic flip mirror. For retinal imaging, an attachment with an additional lens is connected to the handheld scanner to lengthen the optical path, and an additional dispersion compensation unit was used in the reference arm to account for the dispersion of the human eye, as shown in Figure 1. There was a manual dial for compensating for the refractive error of the patient.

Light from a superluminescent diode source (Superlum, Cork, Ireland) with a 70-nm full-width half-maximum (FWHM) spectral bandwidth at a center wavelength of 830 nm is guided into a 2 × 2 fiber coupler and split into sample and reference arms. The reflected signals from each arm are then recombined at the fiber coupler and a custom-designed spectrometer captures the resulting spectral interference.[13] The spectrometer is comprised of a collimator, a diffraction grating with 1200 lines/mm (Wasatch Photonics, Logan, UT), an achromatic doublet lens, and a complementary metal–oxide–semiconductor (CMOS) line scan camera (Sprint, Basler, Ahrensburg, Germany) with 2048 pixels and a 140 kHz line scan acquisition rate. The spectral data from the spectrometer camera are digitized by a frame grabber (National Instruments, Austin, TX), sampled, rescaled as a function of wave number, and visualized after image processing. The size of the handheld scanner is 11.25 × 5 × 10 cm, and the total weight is 600 g, which to our knowledge, makes it both the smallest and the lightest handheld OCT scanner, at time of submission. In clinical practice, the size and weight of the handheld allow for very convenient acquisition of images, with no significant image fluctuations due to polarization dependencies or other artifacts.

Our handheld OCT system has comparable system specifications to that of a leading commercial desktop ophthalmic system (RTVue; Optovue, Inc., Fremont, CA), as shown in Table 1. The commercial desktop system is used primarily in ophthalmology specialist offices to diagnose and track patient disease progression. Both systems have comparable axial resolution, scan range depth, and scan beam wavelength, while
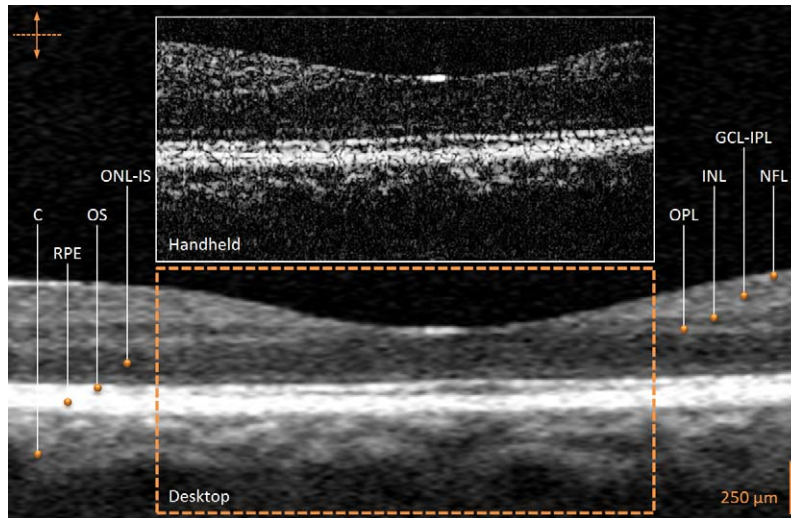
Figure 2. In vivo human retinal OCT images from a healthy volunteer (control) acquired with the handheld scanner and commercial desktop systems. The comparison reveals normal anatomical retinal layers as indicated. The commercial desktop system image was focused on the perifoveal area to facilitate optimal comparison with the handheld system image. No compensation for the refractive index of the tissue imaged was performed in the image from either system to facilitate comparison. The commercial desktop system image was axially scaled to match the 1:1 aspect ratio of the handheld scanner system image and then cropped for image comparison between systems. C, choroid; RPE, retinal pigment epithelium; OS, outer segment layer; ONL-IS, outer nuclear layer/inner segment layer; OPL, outer plexiform layer; INL, inner nuclear layer; GCL-IPL, ganglion cell layer/inner plexiform layer; NFL, nerve fiber layer.

remaining under regulatory optical power exposure limits at the pupil of the eye. Currently, the commercial desktop system has a slightly higher transverse resolution due to proprietary software while the handheld system possesses a significantly faster scan rate. To optimize anatomical feature comparison between systems, the commercial desktop system images were axially scaled to match the 1:1 aspect ratio of the handheld scanner system image, and then cropped to facilitate side-by-side comparison.

This human subjects study was conducted at the Eye Center and the Beckman Institute for Advanced Science and Technology under a protocol approved by the institutional review board at the University of Illinois at Urbana-Champaign, conforming to the Declaration of Helsinki with informed consent from all participants. All images presented here were acquired by an ophthalmologist and retinal specialist (SIS) with the patient in the sitting position and with no additional support provided for the handheld. Comparable images were obtained by technicians, as well as scientists and engineers with no prior medical or surgical training.

Results

Real-time OCT images of both eyes were acquired from six patients exhibiting diabetes-related retinal

pathology. One healthy volunteer was imaged as a control. The control image comparison between the two systems in Figure 2 illustrates the retinal layer substructures including the choroid, retinal pigment epithelium, outer segment layer, outer nuclear layer/inner segment layer, outer plexiform layer, inner nuclear layer, ganglion cell layer/inner plexiform layer, and nerve fiber layer.[33,34] The images captured by the commercial desktop OCT system appear smoothed or averaged with less speckle, following proprietary image processing. This is in contrast to the single, nonaveraged, OCT images acquired by our handheld scanner and system and presented for comparison.

Six patients had their retina in each eye imaged with both OCT systems. In both sets of images, the structural irregularities of the retinal layers could be identified, as seen in Figure 3. The retinal OCT images of patients with nondiabetic (Figs. 3A, 3B) and diabetic (insulin-dependent; Figs. 3C, 3D) retinal edema depict characteristic swollen macula structure due to intraretinal cysts, and similar structures are observed in the images from both the handheld and commercial desktop systems.[35,36] For patients with vitreomacular traction, the posterior vitreous gel forms a strong adhesion to the retina and pulls it forward, often causing retinal distortion, and affecting the patient's vision. These defining
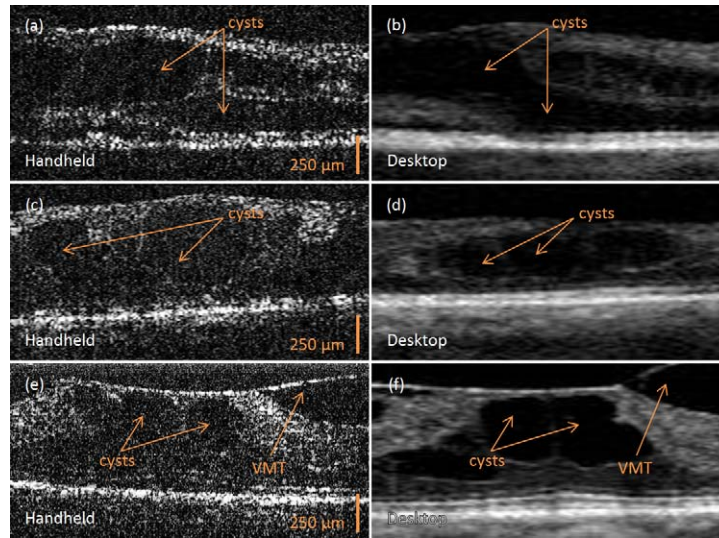
Figure 3. In vivo human OCT images of retinal pathology acquired with the handheld scanner (A, C, E) and commercial desktop (B, D, F) systems. (A, B) Retina with cystic morphology corresponding to retinal edema. (C, D) Retina with cystic morphology corresponding to diabetic retinal edema. (E, F) Retina with vitreomacular traction (VMT) and resultant cystic morphology changes. All commercial desktop system images were focused on the perifoveal area to facilitate optimal comparison with the handheld system images. The commercial desktop system image was axially scaled to match the 1:1 aspect ratio of the handheld scanner system image and then cropped for image comparison between systems.

characteristics of the macula can be visualized (Figs. 3E, 3F) and differentiated from similar looking diagnoses.[36,37]

In Table 2 our handheld OCT system is compared with current commercially-available ophthalmology handheld scanners (iVue; Optovue, Inc. and Envisu C-Class; Bioptigen, Inc., Durham, NC). Our device has a faster scan rate, a lighter, more compact design, and does not require a stand for stabilization. The other scanners have a better depth of resolution.[38,39]

Discussion

This comparison study establishes the ability of our handheld system to acquire patient images quickly, with sufficient resolution and negligible motion artifacts that would normally limit its

Table 2. OCT System Specification Comparison Between Current Commercial Handheld Ophthalmic Systems (iVue, Optovue, Inc.[38] and Envisu C-Class, Bioptigen, Inc.[39]) and Our Handheld OCT Scanner System

	Handheld	iVue	Envisu C2200	Envisu C2300
OCT image (A-scans/sec)	70,422	26,000	32,000	32,000
Frame rate (A-scans/frame)	1,006 (70 frames/sec)	256–1,024 (25–101 frames/sec)	1,024 (31.25 frames/sec)	1,024 (31.25 frames/sec)
Depth resolution, μm	4	5	6 (840 nm) 3 (870 nm)	6 (840 nm) 4 (870 nm)
Transverse resolution, μm	15	15	11	11
Scan range depth, mm	2	2–2.3	1.7	2.5
Scan beam wavelength, nm	830	840	840, 870	840, 870
Weight, kg	0.6	2.2	1.5	1.5
Dimensions, cm (h × w × l)	11.25 × 5 × 10	31.75 × 14.22 × 27.69	18 × 8 × 23	18 × 8 × 23

diagnostic use. This study also demonstrates that our handheld system could be used to identify relevant anatomical structures and pathologies in the eye, potentially enabling earlier screening, disease detection, and treatment.

There are well-known tradeoffs between handheld imaging systems compared with fixed desktop systems. While handheld systems often have more limitations associated with motion artifacts and the need for minimizing hardware to ensure portability, they also enjoy distinct advantages. These include an ability to dynamically and interactively explore areas of interest, a portability that yields a prompt clinical examination for efficient and effective clinical decision making, and the possibility of coupling imaging with therapeutic options, such as delivering laser treatment to visualized areas. There is a long tradition of handheld systems in ophthalmology. The ophthalmoscope that transformed the face of medicine as the first imaging technology that allowed direct visualization of structures inaccessible by other means, such as the vascular system (retinal vessels) and the central nervous system (optic nerve/disk), quickly became a handheld system.[40,41] It remains a handheld system in both direct and indirect forms for primary care physician and specialist alike. In fact, one of the most critical examinations in the ophthalmologist's clinic is an interactive, dynamic examination performed on a patient's dilated eye with a head mounted indirect ophthalmoscope and a handheld 20 diopter lens. OCT technology and handheld OCT systems can potentially play a similarly influential role in the future of medicine.

Improved transverse resolution and a larger field of view (FOV) may allow ophthalmologists some advantage in detecting and monitoring minute differences in the anterior and posterior chamber layers during ocular disease progression. The software for the handheld system can be adapted to process the OCT images to improve the transverse resolution to a degree that is comparable with that of the commercial desktop system.[42–44] However, it is important to note several observations. First, many of the breakthroughs identifying key retinal pathologies were made with early time-domain OCT systems, when the transverse resolutions were modest.[2,35,37] While speed of acquisition is an important factor, particularly for 3D volume acquisition and quantification of clinical ocular characteristics, and while our system's rate is significantly higher than that of the commercial desktop system and that of other handhelds (Tables 1, 2), the fundamental clinical diagnosis of a number of pathologies does not necessarily improve in a linearly proportional way with increased speed or resolution.[3,38,39,45] Second, while increasing the field of view would expose a larger portion of the cornea or retina, it is well established that the most clinically relevant corneal and retinal pathologies lay at the center of each, tipping the FOV-resolution tradeoff toward improved resolution. Clinicopathological examples include the facts that peripheral corneal scars most often go unnoticed by patients and that the retinal cone density drops off dramatically within less than a degree.[46] As demonstrated in the ETDRS study, the diagnosis of clinically-significant macular edema (CSDME) involves the examination of macular areas of diameters varying from 500 to 1500 μm.[17] Third, it is possible to manually and dynamically scan the periphery with the handheld. Finally, added functionality at a significantly higher cost is neither necessary nor appropriate in the context of primary care, where the emphasis lies in screening new patients and monitoring progress in patients with milder expressions of ocular diseases.

Following screening and early disease detection in primary care via our optimized handheld OCT system, patients can be referred to a specialist where more in-depth, clinical examinations can be performed, where higher resolution images via OCT and other modalities can be obtained as needed, and where therapies can be selected and delivered to target the specifically diagnosed condition. While many primary care physicians are adept at using the ophthalmoscope, they can definitely take advantage of more advanced technologies and methods for acquiring critical patient data, as provided by OCT. Our handheld OCT system has the potential to be such a tool without affecting the patient examination pace, and at a fraction of the cost and size of other quantitative imaging instruments. Since our system is portable, a primary care office or multiphysician practice group would ideally only need to purchase one system, which can be moved between examination rooms, much like ultrasound imaging or electrocardiogram (EKG) instruments are used today in these clinics. These advantages can potentially improve the standard quality of primary care, which has long been overlooked for commercial technological advancements in imaging.

This light and fast handheld scanner and accompanying OCT system has the potential to be a flexible and effective tool in the hands of all physicians, and in particular, those at the "front-line" providing screening, early diagnosis, quantitative longitudinal moni-

toring, and prompt intervention to safeguard the health and well-being of patients.

Acknowledgments

Disclosure: **S.I. Sayegh**, None; **R.M. Nolan**, None; **W. Jung**, None; **J. Kim**, None; **D.T. McCormick**, None; **E.J. Chaney**, None; **C.N. Stewart**, None; **S.A. Boppart**, Co-Founder and Chief Medical Officer of PhotoniCare, Inc.

References

1. Huang D, Swanson EA, Lin CP, et al. Optical coherence tomography. *Science*. 1991;254:1178–1181.
2. Puliafito CA, Schuman JS, Fujimoto JG. Optical coherence tomography of ocular diseases. 1st ed. Thorofare, NJ: Slack, Inc.; 1995.
3. Schuman JS, Puliafito CA, Fujimoto JG, Duker JS. Optical coherence tomography of ocular diseases. 3rd ed. Thorofare, NJ: Slack, Inc.; 2013.
4. Christopoulos V, Kagemann L, Wollstein H, et al. In vivo corneal high-speed, ultra-high-resolution optical coherence tomography. *Arch Ophthalmol*. 2007;125:1027–1035.
5. Srinivasan VJ, Monson BK, Wojtkowski M, et al. Characterization of outer retinal morphology with high-speed, ultrahigh-resolution optical coherence tomography. *Invest Ophthalmol Vis Sci*. 2008;49:1571–1579.
6. Kim JS, Ishikawa H, Sung KR, et al. Retinal nerve fibre layer thickness measurement reproducibility improved with spectral domain optical coherence tomography. *Br J Ophthalmol*. 2009; 93:1057–1063.
7. Pan Y, Xie H, Fedder GK. Endoscopic optical coherence tomography based on a mirror. *Opt Lett*. 2001;26:1966–1968.
8. Zara JM, Yazdanfar S, Rao KD, Izatt JA, Smith SW. Electrostatic micromachine scanning mirror for optical coherence tomography. *Opt Lett*. 2003;28:628–630.
9. Jung W, McCormick DT, Zhang J, Wang L, Tien NC, Chen Z. Three-dimensional endoscopic optical coherence tomography by use of a two-axis microelectromechanical scanning mirror. *Appl Phys Lett*. 2006;88:163901–163903.
10. Kim KH, Park BH, Maguluri GN, et al. Two-axis magnetically-driven MEMS scanning catheter for endoscopic high-speed optical coherence tomography. *Opt Express*. 2007;15:18130–18140.
11. Gilchrist KH, McNabb RP, Izatt JA, Grego S. Piezoelectric scanning mirrors for endoscopic optical coherence tomography. *J Micromech Microeng*. 2009;19:095012.
12. Sun J, Xie H. MEMS-based endoscopic optical coherence tomography. *Int J Opt*. 2011;1:1–12.
13. Jung W, Kim J, Jeon M, Chaney EJ, Stewart CN, Boppart SA. Handheld optical coherence tomography scanner for primary care diagnostics. *IEEE*. 2011;58:741–744.
14. Nguyen CT, Jung W, Kim J, et al. Noninvasive in vivo optical detection of biofilm in the human middle ear. *PNAS*. 2012;109:9529–9534.
15. Boyle JP, Thompson TJ, Gregg EW, Barker LE, Williamson DF. Projection of the year 2050 burden of diabetes in the US adult population: dynamic modeling of incidence, mortality, and prediabetes prevalence. *Popul Health Metr*. 2010; 8:1–12.
16. Department of Health and Human Services. *National diabetes fact sheet: national estimates*

and general information on diabetes and prediabetes in the United States. 2011. Atlanta, GA: U.S. Centers for Disease Control and Prevention; 2011.

17. Kinyoun J, Barton F, Fisher M, Hubbard L, Aiello L, Ferris F. Detection of diabetic macular edema. Ophthalmoscopy versus photography–Early Treatment Diabetic Retinopathy Study Report Number 5. The ETDRS Research Group. Ophthalmology. 1989;96:746–750.

18. Nguyen QD, Brown DM, Marcus DM, et al; for the RISE and RIDE Research Group. Ranibizumab for diabetic macular edema–results from 2 phase III randomized trials: RISE and RIDE. Ophthalmology. 2012;119:789–801.

19. Yang CS, Cheng CY, Lee FL, Hsu WM, Liu JH. Quantitative assessment of retinal thickness in diabetic patients with and without clinically significant macular edema using optical coherence tomography. Acta Ophthalmol Scand. 2001; 79:266–270.

20. Wilkinson CP, Ferris FL III, Klein RE, et al; for the Global Diabetic Retinopathy Project Group. Proposed international clinical diabetic retinopathy and diabetic macular edema disease severity scales. Ophthalmology. 2003;110:1677–1682.

21. Brown JC, Solomon SD, Bressler SB, Schachat AP, DiBernardo C, Bressler NM. Detection of diabetic foveal edema: contact lens biomicroscopy compared with optical coherence tomography. Arch Ophthalmol. 2004;122:330–335.

22. Virgili G, Menchini F, Dimastrogiovanni AF, et al. Optical coherence tomography versus stereoscopic fundus photography or biomicroscopy for diagnosing diabetic macular edema: a systematic review. Invest Ophthalmol Vis Sci. 2007;48:4963–4973.

23. Bressler NM, Miller KM, Beck BW, et al. Observational study of subclinical diabetic macular edema. Eye. 2012;26:833–840.

24. Byeon SH, Chu YK, Hong YT, Kim M, Kang HM, Kwon OW. New insights into the pathoanatomy of diabetic macular edema: angiographic patterns and optical coherence tomography. Retina. 2012;32:1087–1099.

25. Vitale S, Ellwein L, Cotch MF, Ferris FL III, Sperduto R. Prevalence of refractive error in the United States. 1999-2004. Arch Ophthalmol. 2008; 126:1111–1119.

26. Solomon KD, Fernández de Castro LE, Sandoval HP, et al; for the Joint LASIK Study Task Force. LASIK world literature review: quality of life and patient satisfaction. Ophthalmology. 2009;116: 691–701.

27. Melki SA, Azar DT. LASIK complications: etiology, management, and prevention. Surv Ophthalmol. 2001;46:95–116.

28. Knorz MC. Flap and interface complications in LASIK. Curr Opin Ophthalmol. 2002;13:242–245.

29. Randleman JB, Shah RD. LASIK interface complications: etiology, management, and outcomes. J Refract Surg. 2012;28:575–586.

30. Avila M, Li Y, Song JC, Huang D. High-speed optical coherence tomography for management after laser in situ keratomileusis. J Cataract Refract Surg. 2006;32:1836–1842.

31. Zhang XX, Zhong XW, Wu JS, et al. Corneal flap morphological analysis using anterior segment optical coherence tomography in laser in situ keratomileusis with femtosecond lasers versus mechanical microkeratome. Int J Ophthalmol. 2012;5:69–73.

32. Optovue, Inc. RTVue brochure. Rev. A. Fremont, CA. 2012; P/N 300-42876.

33. Mishra A, Wong A, Bizheva K, Clausi DA. Intraretinal layer segmentation in optical coherence tomography images. Opt Express. 2009;17:23719–23728.

34. Garvin MK, Abramoff MD, Kardon R, Russell SR, Wu X, Sonka M. Intraretinal layer segmentation of macular optical coherence tomography images using optimal 3-D graph search. IEEE Trans Med Imaging. 2008;27:1495–1505.

35. Hee MR, Puliafito CA, Duker JS, et al. Topography of diabetic macular edema with optical coherence tomography. Ophthalmology. 1998;105:360–370.

36. Srinivasan VJ, Wojtkowski M, Witkin AJ, et al. High-definition and 3-dimensional imaging of macular pathologies with high-speed ultrahigh-resolution optical coherence tomography. Ophthalmology. 2006;113:2054.e1–2054.e14.

37. Sulkes DJ, Ip MS, Baumal CR, Wu HK, Puliafito CA. Spontaneous resolution of vitreomacular traction documented by optical coherence tomography. Arch Ophthalmol. 2000;118:286–287.

38. Optovue, Inc. iVue SD-OCT. Rev. E. Fremont, CA. 2013; P/N 300-45927.

39. Bioptigen, Inc. Envisu C-Class System Comparison. Available at: http://www.bioptigen.com/products/r-class/system-comparison/. Accessed 15 March 2013.

40. von Helmholtz, H. Beschreibung eines Augen-Spiegels: zur Untersuchung der Netzhaut im lebenden Auge. Berlin: A. Forstner'sche Verlagsbuchhandlung; 1851.

41. Anagnostakis, A. Essai sur l'exploration de la rétine et des milieux de l'oeil sur le vivant, au

moyen d'un nouvel ophthalmoscope. Paris: Rignoux; 1854.

42. Ralston TS, Marks DL, Carney PS, Boppart SA. Interferometric synthetic aperture microscopy. *Nat Phys*. 2007;3:129–134.

43. Ralston TS, Marks DL, Carney PS, Boppart SA. Real-time interferometric synthetic aperture microscopy. *Opt Express*. 2008;16:2555–2569.

44. Ralston TS, Adie SG, Marks DL, Boppart SA, Carney PS. Cross-validation of interferometric synthetic aperture microscopy and optical coherence tomography. *Opt Letters*. 2010;35:1683–1685.

45. Sayegh SI. OCT corneal topography within ¼ diopter in the presence of saccadic eye movements. *Proc. SPIE* Optical Coherence Tomography and Coherence Domain Optical Methods in Biomedicine XVII. 2013; 8571:85713D–85713D7.

46. Osterberg G. Topography of the layer of rods and cones in the human retina. *Acta Ophthalmol Suppl*. 1935;6:1–103.

translational vision science & technology